PULSED TERAHERTZ GENERATION BY A FEMTOSECOND LASER AND ITS APPLICATIONS

Yun-Sik Jin, Seok-Gy Jeon, Geun-Ju Kim, Chae-Hwa Shon, Sun-Shin Jung
Korea Electrotechnology Research Institute (KERI)
28-1, Sung-Ju Dong, Changwon Gyungnam, 641-120, Korea
E-mail: ysjin@keri.re.kr

1.Introduction

During past ten years, there has been considerable progress in the generation and detection of terahertz (THz) sub-millimeter waves (note: 1 THz correspond to 300 μm, vacuum wavelength). Research interest in terahertz waves stems from the broadband pulsed nature of the radiation and the THz-frequency response of materials, ranging from semiconductor to human tissue. The THz regime is populated by the rotational and vibrational energy states of polar molecules, either in liquid or gas form. Using T-ray transmission and reflection spectroscopy, samples from gas to the solid state can be completely characterized at THz frequencies. The frequency-dependent absorption and dispersion of materials (e.g. measurement of complex dielectric constant) in the millimeter to sub-millimeter spectral range can be obtained by THz-TDS [1]. The THz pulses have also been used for the imaging application (T-ray imaging) of various materials including dielectric, semiconductor and biomedical tissues [2].

Photoconductive antenna, nonlinear effect of optical rectification and surface field of semiconductor are the most widely used laser-based techniques of pulsed THz generation and detection. These are methods of producing an ultra-fast current or polarization transients, which acts as a broadband sources as predicted in Hertz's equation [3-5].

In this paper, generation and detection of ultra-wideband THz pulse by the photoconductive antenna, optical rectification and semiconductor surface was described. Variation of THz electric field with some parameter was investigated. As application examples, solid gun propellants have been analyzed by a terahertz time domain spectroscopy (THz TDS). The imaging capability of THz measurement system was verified by imaging a cloverleaf and watermark image of money.

2. Pulsed terahertz wave generation and detection

Three major methods for pulsed THz radiation via a femtosecond laser were shown schematically in Fig. 1. The laser source is a commercial mode-locked Ti:sapphire laser (Spectra Physics Mai Tai) producing 70-120 fs pulses at 780-920 nm with a repetition rate of 80 MHz and an average power of 600-1200 mW. We used general setup of terahertz generation and detection scheme [6]. The fs laser beam was divided into two beams, one for exciting the emitter antenna, ZnTe crystal and InAs semiconductor (pump beam), and the other for measuring the THz signal at the detector antenna (probe beam), by a beam splitter. The fs pump pulses were focused on target material by an objective lens (f = 40 mm). An aplanatic hyper-hemispherical silicon lens is attached to the back of the THz emitter and detector to increase the coupling efficiency of THz pulse from the antenna to free space and the quality of THz beam for the following optics. The detector antenna was gated by fs probe beam pulses that were separated from pump beam pulse by the beam splitter. To increase the signal-to-noise ratio, the pump beam was modulated with a mechanical chopper at

ISBN: 89-86522-79-9 94460©KEES

1.5kHz. The output signal from the detector antenna was monitored with a lock-in amplifier.

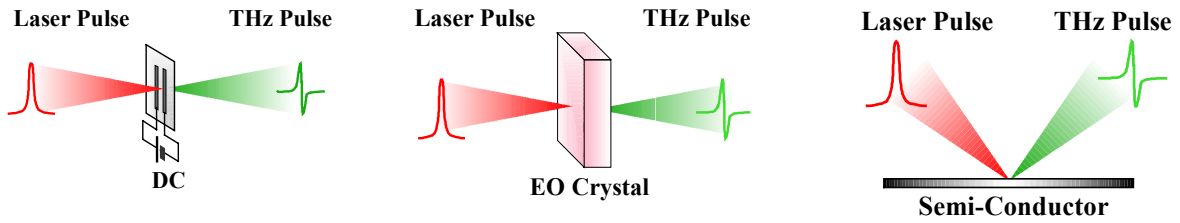

(a) photoconductive antenna (b) optical rectification (c) semiconductor surface

Fig. 1. Schematic diagram of three major methods of pulsed THz generation

A. Photoconductive Antenna (PCA) Method

The emitter and detector antennas are fabricated on a low temperature grown GaAs (LT-GaAs) wafer. The coplanar metal strip lines of antennas consist of Au/Ni thin film with a thickness of 3000 Å. The gap distance of emitter and detector antenna was 200 μm and 5 μm, respectively. The time domain waveform and frequency domain spectrum of THz pulse from the PCA is shown in Fig. 2 (a). The bias voltage between coplanar stripline of emitter antenna was 100 V (E_{bias} = 5 kV/cm), and the laser power of pump and probe beam was 10 mW. The signal to noise ratio (SNR) of the THz waveform was estimated to be as high as 1000. The spectral distribution is centered near 0.3 - 0.5 THz, and extend near to 3 THz. The full width at half maximum (FWHM) of the spectrum was estimated as about 1 THz. The THz electric field increased linearly with the bias voltage between antenna electrodes (Fig. 2 (b)). The breakdown voltage of the emitter antenna limits the availability of the highest THz radiation field. Above bias voltage of 240 V(E_b=12 kV/cm) at the pump power of 20 mW, the damage of the emitter antenna was occurred. Fig. 2 (c) shows the variation of THz field with wavelength of pump laser. The wavelength was scanned from 780 nm to 900 nm. We can see an abrupt decrease of THz signal above 860 nm, which means that the pumping efficiency decease when the photon energy of pump laser is lower than the band gap energy of a GaAs semiconductor (E_g of GaAs: 1.43 eV=867 nm).

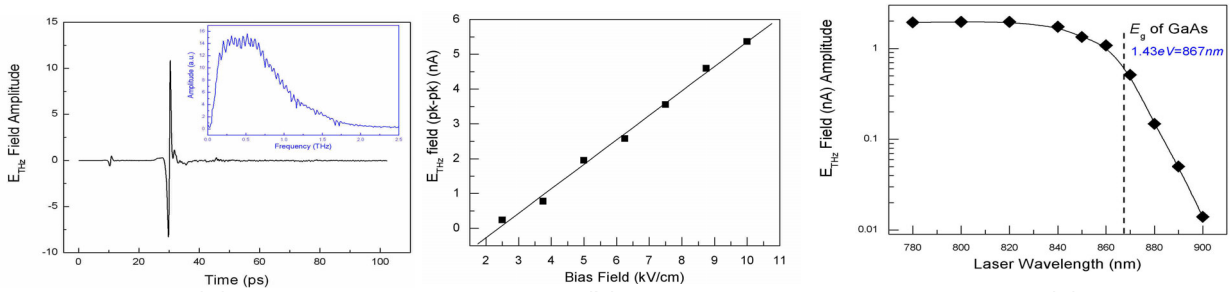

(a) (b) (c)

Fig. 2 (a) Typical THz waveform and spectrum generated by PCA, (b) bias voltage dependency, (c) pump laser wavelength dependency

B. Optical Rectification (OR) Method

The most popular electro-optical material for optical rectification (OR) is ZnTe, because of its physical durability and excellent phase matching [7]. We used 1mm thick ZnTe (110) crystal for OR. Fig. 3 (a) shows THz waveform obtained by OR. The pump and probe laser power were 100 mW and 10 mW, respectively. Fig. 3 (b) illustrates the variation of THz field intensity as a function of the pump laser power. At low power level, the THz signal showed a quadratic increase and at higher laser power above 50 mW, the THz field increased linearly. The bandwidth of THz radiation by OR depends on the duration of the optical pulse width. With the fs laser we used, one can change the pulse width from 70 fs to 100 fs by tuning the oscillating wavelength from 800nm to 900 nm. The THz pulse bandwidth variation with wavelength (or pulse width) of the pump laser was shown in Fig. 3 (c). As the laser

wavelength or pulse width increases, the bandwidth of THz spectrum showed a sharp decrease.

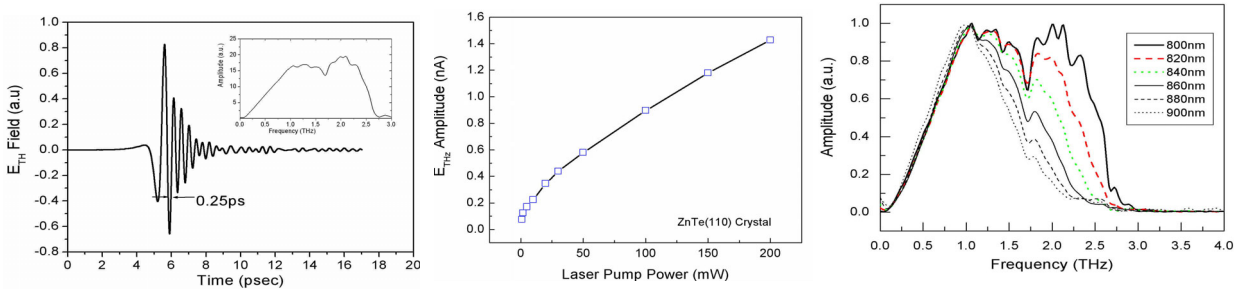

(a) (b) (c)

Fig. 3 (a) Typical THz pulse waveform and spectrum generated by OR, (b)pump power dependency, (c) pump laser wavelength dependency

C. Generation of THz radiation from Bare Semiconductor Surface

Thz radiation can be generated by the acceleration of photoexcited electron-hole pairs in semiconductor surfaces. Ultrafast charge transport can be driven by both the intrinsic electric field perpendicular to the semiconductor surface and by differences in the electron and hole mobilities (photo-Dember effect) [8]. The excitation pulse illuminated the surface of (100) InAs wafer at an incident angle of 45 degrees with respect to surface normal. The p- and n-type InAs wafer with a carrier concentration of $1x10^{16}$ cm^{-3} at room temperature were used as the medium. Fig. 4 (a) and (b) shows the typical waveforms and spectra of THz pulse generated from p- and n-type InAs surface, respectively. No significant difference was observed between these two types of semiconductor. The spectral distribution is centered near 0.8 - 1.2 THz, and extend near to 4THz. The full width at half maximum (FWHM) of the spectrum was estimated as about 1.5 THz. At low power level, the THz signal showed a quadratic increase and at higher laser power above 100 mW, the THz field increased linearly, similar to optical rectification case (Fig. 4 (c)).

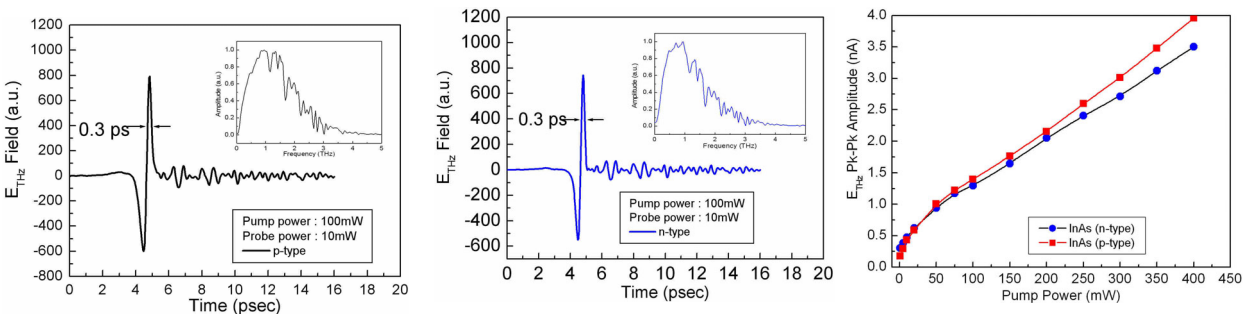

(a) (b) (c)

Fig. 4 Typical THz pulse waveform and spectrum generated by p-type (a) and n-type (b) InAs semiconductor, (c) pump power dependency

3. Application of THz Pulse in THz-TDS and T-Ray Imaging

THz spectroscopy is an attractive non-contact, non- destructive and safe technology that has been applied to detect and identify many dangerous explosive materials. We investigated the ability of THz-TDS to identify solid gun propellants. Two solid propellants of JA2 and LOVA were chosen. JA2 propellant is currently utilized in US 120 mm gun systems and LOVA propellant is a newly developed propellant, which will be used to electro-thermal chemical (ETC) gun [9]. The propellants were sliced into 1 mm thickness samples. Fig. 5 (a), (b), (c) shows transmission mode THz TDS results of the propellants. Both the sample showed strong absorption in THz range. JA2 and LOVA have very different absorption spectra in the frequency range between 0.1 and 1.5 THz. Especially, LOVA propellant showed strong absorption peak near 0.8 THz. From the above results, we believe that there are good prospects for using T-rays to identify various propellants.

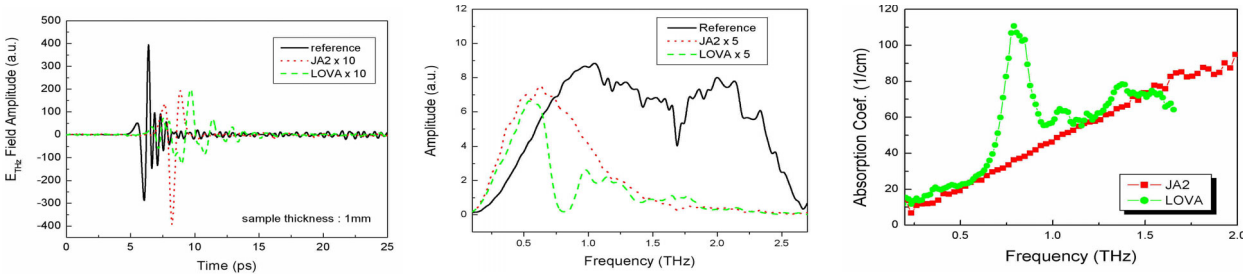

(a) Temporal THz waveform (b) FFT spectra (c) Calculated absorption coefficient

Fig. 5 THz TDS of solid gun propellants

We have obtained THz images of a cloverleaf and the watermark on Korean 10,000 Won note. Fig. 6 (a) shows the T-Ray image of a live cloverleaf. The contrast was obtained by the position of peak. In case of the imaging of watermark (Fig. 6 (b)), intensity difference of transmitted THz pulse at every pixel was used to construct the image. During the whole scanning process (scan step: 250 μm), the timing of the optical delay line is set at the peak position of it. In Fig. 6(b) of constructed THz image, we can see clearly the hidden watermark on the currency.

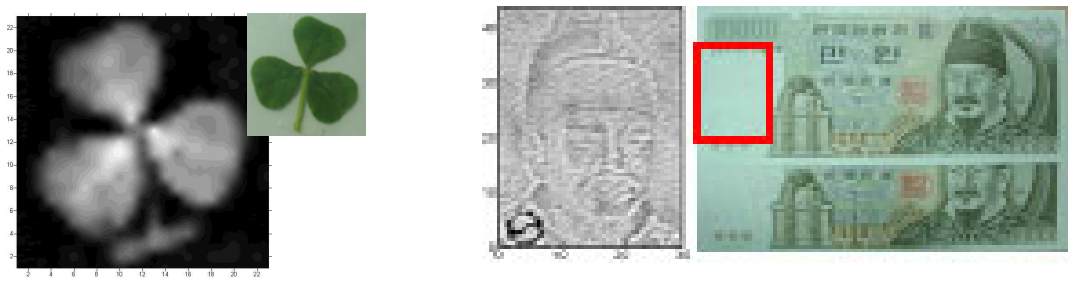

(a) (b)

Fig. 6 THz image of a live cloverleaf (a) and watermark on 10,000 Korean Won note (b).

4. Summary

We have demonstrated pulsed THz generation from PCA, OR and semiconductor surface excited by ultra-fast optical pulses. Radiation characteristics of each method have been investigated. As application examples, gun propellants have been analyzed by THz-TDS and a cloverleaf and watermark of 10,000 Korean Won paper was imaged successfully.

References

[1] L. Duvillaret, F. Garet, and J. J. Coutaz, IEEE J. Selected Topics in Quantum Electron., **2** (1996) 739
[2] D. M. Mittleman, M. Gupta, R. Neelamani, R. G. Baraniuk, J. V. Rudd, and M. Koch, Appl. Phys. **B 68** (1999) 1085
[3] D. H. Auston and K. P. Cheung and P. R. Smith, Appl. Phys. Lett., **45(6)** (1984) 284
[4] P. R. Smith, D. H. Auston, and M. C. Nuss, IEEE J. Quantum Electron. **24** (1988) 255
[5] B. B. Hu, X.-C. Zhang, Appl. Phys. Lett., **56(6)** (1991) 25
[6] B. Ferguson and X, -C. Zhang, Nature materials. **1** (2002) 26
[7] A. Rice, Y. Jin, X. F. Ma, X. -C. Zhang, D. Bliss, J. Larkin and M. Alexander. Appl. Phys. Lett. **64** (1994) 1324 6
[8] H. TAKAHASHI, A. QUEMA, M. GOTO, S. ONO and N. SARUKURA, Jpn. J. Appl. Phys. **42** (2003) L 1259
[9] G. P. Wren and W. F. Oberle, IEEE Trans. Magn. 37 (2001) 211